

PUBLISHED VERSION

Afshar Vahid, Shakraam; Ferrier, G. A.; Bao, Xiaoyi; Chen, L.
Effect of the finite extinction ratio of an electro-optic modulator on the performance of distributed probe-pump Brillouin sensorsystems, *Optics Letters*, 2003; 28 (16):1418-1420.

Copyright © 2003 Optical Society of America

PERMISSIONS

http://www.opticsinfobase.org/submit/review/copyright_permissions.cfm#posting

This paper was published in *Optics Letters* and is made available as an electronic reprint with the permission of OSA. The paper can be found at the following URL on the OSA website <http://www.opticsinfobase.org/abstract.cfm?URI=ol-28-16-1418>. Systematic or multiple reproduction or distribution to multiple locations via electronic or other means is prohibited and is subject to penalties under law.

OSA grants to the Author(s) (or their employers, in the case of works made for hire) the following rights:

(b)The right to post and update his or her Work on any internet site (other than the Author(s') personal web home page) provided that the following conditions are met: (i) access to the server does not depend on payment for access, subscription or membership fees; and (ii) any such posting made or updated after acceptance of the Work for publication includes and prominently displays the correct bibliographic data and an OSA copyright notice (e.g. "© 2009 The Optical Society").

17th December 2010

<http://hdl.handle.net/2440/33951>

Effect of the finite extinction ratio of an electro-optic modulator on the performance of distributed probe-pump Brillouin sensor systems

Shahraam Afshar V., Graham A. Ferrier, Xiaoyi Bao, and Liang Chen

Fiber Optics Group, Department of Physics, University of Ottawa, 150 Louis Pasteur, Ottawa, Ontario K1N 6N5, Canada

Received March 12, 2003

The effect of the finite extinction ratio of an electro-optic modulator (EOM) on the Brillouin frequency measurement of a distributed Brillouin-based fiber optic sensor is studied. An EOM with a finite extinction ratio limits the application of Brillouin optical time domain analysis in a distributed Brillouin-based fiber optic sensor. This results in confusion in specifying the location of the strained region and in error in detecting the Brillouin frequency and hence in strain and temperature measurement. © 2003 Optical Society of America
OCIS codes: 290.5830, 060.4370, 060.2370.

Brillouin-scattering-based fiber optic sensors are based on a nonlinear optical phenomenon called stimulated Brillouin scattering. A sensor configuration developed by Bao *et al.*¹ monitors the interaction of two counterpropagating laser beams, a cw pump and a pulsed Stokes beam, through an induced acoustic wave inside the fiber. The interaction magnifies the pulsed Stokes beam at the expense of depleting the pump beam, which is then detected as a loss signal, as shown in Fig. 1. The largest depletion of the pump beam at a point along the fiber, i.e., at resonance, happens when the frequency of the acoustic wave ν_B at that point matches the beat frequency of the two laser beams, i.e., $\nu_p - \nu_s = \nu_B$, where ν_p and ν_s are the pump and the Stokes frequencies, respectively. The frequency of the acoustic wave, hereafter called the Brillouin frequency, is related to the fiber properties and to the pump wavelength and varies linearly with temperature and strain.² By scanning Stokes frequency ν_s over a range of frequencies and measuring the intensity of the corresponding signal at the detector, one obtains a Brillouin loss spectral profile. The amount of shift in the resonance frequency of this profile, $\delta\nu_B$, with respect to a reference condition is used to determine temperature or strain variations. These distributed sensors can measure, in principle, strain and temperature at any point along the sensing fiber. Distributed sensing is possible through Brillouin optical time-domain analysis (BOTDA). In this method the spatial information is related to the round-trip time by $z = tc/(2n)$. This means that the signal detected at time t represents the Stokes-pump interaction at position $z = tc/(2n)$ and time $t/2$. Consequently the spatial resolution is determined by $\delta z = cW/(2n)$, where W is the Stokes pulse width.

In the setup developed by Bao *et al.*,¹ an electro-optic modulator was used to convert a cw laser beam into a pulsed laser beam with a controllable pulse width. However, because the electro-optic modulator has a finite extinction ratio, defined as $R_x = (P_{\text{pulse}} + P_{\text{cw}})/P_{\text{cw}}$, the pulsed laser always contains a cw component, which is hereafter called leakage. We have developed a simulation model of Brillouin-based fiber optic sensors and found that the finite extinction ratio affects the Brillouin spectral shape and

limits the ability of BOTDA to obtain the spatial information.³ Consequently, the Brillouin interaction of the Stokes and the pump beams consists of both leakage-pump and pulse-pump interactions. The dominant interaction ultimately determines the resultant profile shape, linewidth, and limitation in obtaining the spatial information. In terms of the overall Brillouin profile, the leakage-pump interaction contributes a Lorentzian distribution, whereas the pulse-pump interaction contributes a Gaussian distribution when the pulse width approaches or narrows below the phonon lifetime.³ In this Letter we demonstrate how the finite extinction ratio limits the capability of BOTDA and how one can minimize this limitation by varying the leakage and Stokes powers and the fiber length. The simulation is based on a numerical model of stimulated Brillouin scattering developed by Afshaarvahid *et al.*,⁴ in which three coupled differential equations,⁵

$$\left(\frac{\partial}{\partial z} - \frac{n}{c} \frac{\partial}{\partial t}\right)E_p = ig_1QE_s + 1/2\alpha E_p, \quad (1a)$$

$$\left(\frac{\partial}{\partial z} + \frac{n}{c} \frac{\partial}{\partial t}\right)E_s = -ig_1Q^*E_p - 1/2\alpha E_s, \quad (1b)$$

$$\left(\frac{\partial}{\partial t} + \Gamma\right)Q = -ig_2E_pE_s^*, \quad (1c)$$

that describe pump E_p , Stokes E_s , and acoustic Q fields are solved numerically. Here g_1 and g_2 are

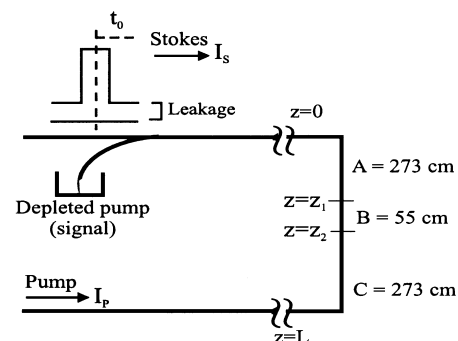


Fig. 1. Geometry used for simulating Brillouin-based fiber optic sensors. The relative Brillouin shifts of regions A, B, and C are 0, -31.9, and 31.9 MHz, respectively.

the coupling coefficients related to the Brillouin signal gain through $g_B = 2g_1g_2/\Gamma$. Γ is a complex value given by $\Gamma = \Gamma_1 + i\Gamma_2$, where $\Gamma_1 = 1/(2\tau)$ is the damping rate and $\Gamma_2 = \Delta\omega = \omega - \omega_B$ is the detuning frequency. We used the geometry shown in Fig. 1 and the following parameters in our model: $g_B = 5 \times 10^{-3}$ cm/MW, $\tau = 10$ ns, $d = 9$ μ m, $W = 1$ ns, $L = 6$ m, $P_{\text{pump}} = 5$ mW, and $P_{\text{pulse}} = 2$ mW, where τ is the phonon lifetime and d is the fiber core's diameter. The input Stokes is a super-Gaussian pulse with a cw leakage component. The sensing fiber consists of three sections: section A, $0 < z < z_1$, is under no strain and has no temperature change and thus no relative Brillouin shift; section B, $z_1 < z < z_2$, is under strain with a relative Brillouin frequency shift of -31.9 MHz; and section C, $z_2 < z < L$, is under strain with a relative Brillouin frequency shift of 31.9 MHz.

Figure 2 shows the frequency profile that corresponds to the middle of section B for several extinction ratios. The $R_x = \infty$ (cw leakage is zero) curve shows a broad Gaussian profile as a result of a short ($W = 1$ ns $< \tau$) pulse-pump interaction. The other profiles, however, show twofold spectral profiles that consist of the Gaussian profile of $R_x = \infty$, indicating their pulse-pump interaction, plus a narrower Lorentzian profile, representing their cw leakage-pump interaction. Therefore the total spectral shape and linewidth of any Stokes-pump interaction are determined by the dominant process of the pulse-pump or leakage-pump interactions. A dominant pulse-pump or leakage-pump interaction makes the Brillouin spectral profile become more Gaussian with a large linewidth or more Lorentzian with a narrower linewidth, respectively. This twofold structure has been observed experimentally and has led to a new spectral fitting method⁶ in which a combination of Gaussian and Lorentzian profiles with different linewidths is used to fit the experimental data. Zooming in on the central part of Fig. 2 reveals (see Fig. 3) that, although the profile corresponds to the middle of section B and hence should present only one peak at the Brillouin frequency shift of -31.9 MHz (peak 1), it presents three peaks, at -31.9 , 0 , and 31.9 MHz, corresponding to the Brillouin frequency shifts of all three sections. This causes confusion in determining the true Brillouin frequency shift of strained section B and errors when the Brillouin frequency shifts of neighboring sections are close to that of this section. The concept of BOTDA is based on the fact that the signal detected at time t represents the Stokes-pump interaction at time $t/2$ and position $z = tc/(2n)$ (assume that z is in region B). An electro-optic modulator with a finite extinction ratio permits cw leakage in every section of the fiber, which complicates the BOTDA measurement in two ways: First, before the Stokes-pump interaction at $t/2$ and $z = tc/(2n)$, the pump is depleted by the cw leakage during time interval $[0, t/2]$. Hence it carries information on the Brillouin interaction in region C. Second, after the pulse-pump interaction at z , the depleted pump continues to interact with the cw leakage component as it propagates in region A

toward the detector. Therefore the signal detected at time t carries the Brillouin interaction information of position z as well as of regions A and C.

The strength of these extra leakage-pump interactions decreases as the leakage power decreases or the pulse power increases (i.e., the extinction ratio increases). This can be seen from Figs. 3 and 4, where we have compared the spectral profiles for several extinction ratios that we obtained by changing the leakage or pulse powers, respectively. We have also compared the height of the Brillouin peak that corresponds to strained section B (peak 1 in Figs. 3 and 4) with those of neighboring peaks 2 and 3 for different extinction ratios. Figure 5 shows that, as the extinction ratio increases, the relative height of peak 1 with respect to those of peaks 2 and 3 increases, resulting in better suppression of peaks 2 and 3. The strength of leakage-pump interactions in regions A and C also depends on the lengths of these regions.

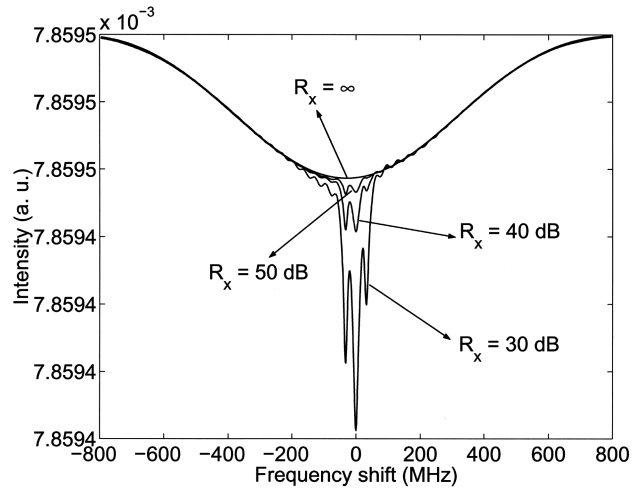


Fig. 2. Brillouin spectral profiles of signals corresponding to the middle of region B for extinction ratios 30, 40, and 50 dB and ∞ .

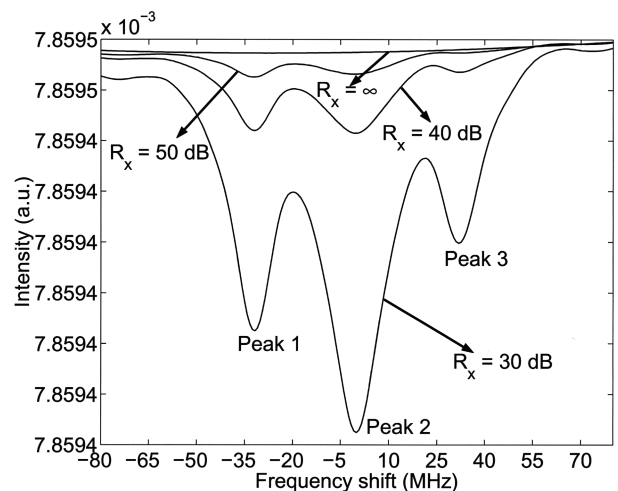


Fig. 3. For all profiles except $R_x = \infty$ there are three peaks, at -31.9 , 0 , and 31.9 MHz. These peaks represent the Brillouin frequency shifts of regions B, A, and C, respectively.

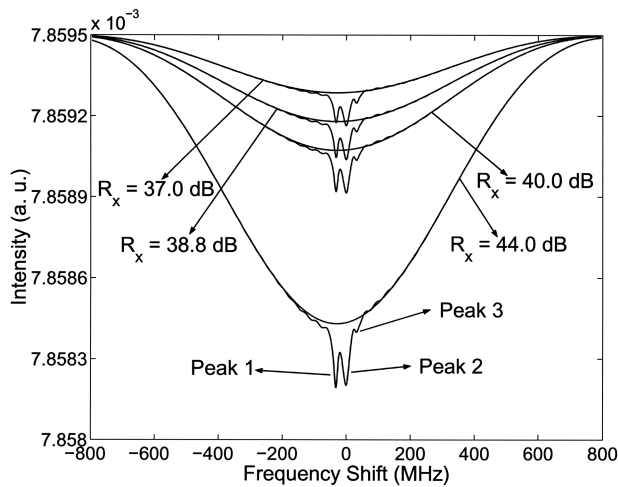


Fig. 4. Brillouin profiles of region B for several extinction ratios that we obtained by varying the pulse component of the Stokes beam.

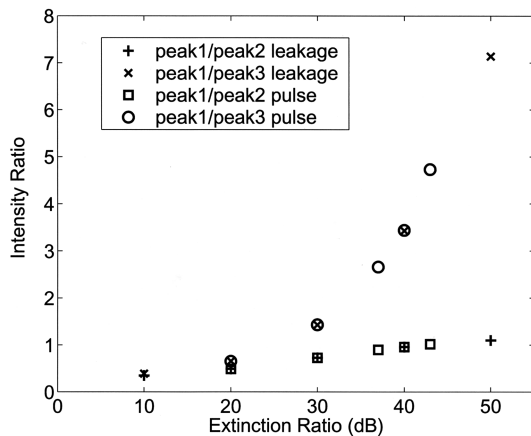


Fig. 5. Relative heights of peak 1–peak 2 and peak 1–peak 3 for several extinction ratios that we achieved by varying the leakage or pulse powers.

Thus the capability of our sensing system to detect the true Brillouin frequency shift of a strained region (e.g., region B) depends on the region's length relative to those of other fiber sections. Figure 6 shows that the height of the true Brillouin peak of strained region B decreases relative to those of regions A and C as their lengths are increased. Therefore, smaller

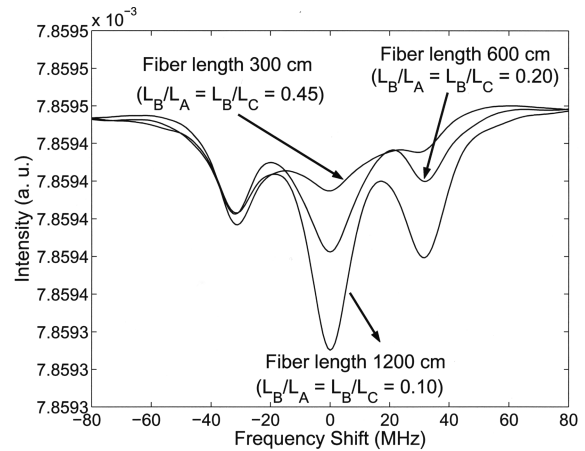


Fig. 6. Brillouin profile for three fiber lengths. The length of region B is constant at 55 cm.

relative lengths L_B/L_A and L_B/L_C lead to greater difficulty in detecting the true Brillouin frequency shift. This means that the best achievable spatial resolution of the sensor system is limited by the fiber length as a result of the extra leakage–pump interactions in regions A and C. As a result, the spatial resolution should be determined by the minimum detectable strain–temperature section rather than by the 10–90% rise time of the pulse, as normally defined in the distributed sensor field.

S. Afshar V.'s e-mail address is safshar@uottawa.ca.

References

1. X. Bao, D. J. Webb, and D. A. Jackson, *Opt. Lett.* **18**, 1561 (1993).
2. T. Kurashima, T. Horiguchi, and M. Tateda, *Appl. Opt.* **29**, 2219 (1990).
3. S. Afshar V., G. A. Ferrier, X. Bao, and L. Chen, "Brillouin spectral characterization of probe–pump distributed fiber optic sensors in the transient regime," submitted to *J. Lightwave Technol.*
4. S. Afshaarvahid, V. Devrelis, and J. Munch, *Phys. Rev. A* **57**, 3961 (1998).
5. G. P. Agrawal, *Nonlinear Fiber Optics* (Academic, San Diego, Calif., 1995).
6. G. A. Ferrier, S. Afshar V., X. Bao, and L. Chen, "New spectral fitting method for distributed Brillouin sensing in the transient regime," submitted to *J. Lightwave Technol.*